Study of a strongly damped collision between heavy ions

M. Zielińska-Pfabé
Smith College, Northampton, Massachusetts 01063

J. Stryjewski
Nicols Research Corporation, Kennedy Space Center, Cape Canaveral, Florida 32920

D. Sperber
Renesselaer Polytechnic Institute, Troy, New York 12180

Ch. Grégoire
Atomic Energy Comission, Paris, France

(Received 24 October 1991; revised manuscript received 29 December 1992)

We present a dynamical analysis of deep inelastic collisions between two ^{98}Mo ions at $E_{c.m.} = 14.7$ MeV/nucleon using two different models. The first, a microscopic model, is based on the Landau-Vlasov equation which includes a two-body residual-interaction collision term. The second model is based on a macroscopic approach which uses collective shape degrees of freedom and a one-body dissipation mechanism. The results of our microscopic calculations show good qualitative agreement with experimental data.

PACS number(s): 25.70.Lm, 24.10.−i

I. INTRODUCTION

In recent years a considerable effort has been devoted to the study of heavy ion collisions at intermediate energies. Experiments performed in this energy range show that one is dealing with highly dissipative processes. Therefore, the results of the analysis of the empirical data depend strongly on the assumed mechanism of the dissipative process. It is then very important to study the first and second moments of the experimentally observed distributions using different approaches to the process of energy dissipation. In this paper we present an investigation of deep inelastic scattering for the reaction ^{98}Mo + ^{98}Mo at a center-of-mass energy of 14.7 MeV per nucleon. Most of our calculations were performed using a semiclassical microscopic model where we solve the Landau-Vlasov equation using a phenomenological collision term [1]. We use a method described in Ref. [2] to determine the second moments of several experimentally interesting distributions. For comparison we have also performed calculations of the first moments using a classical macroscopic model which is based on a shape parametrization of the mean field [3] and includes one-body wall and window dissipation.

The standard starting point for a quantum microscopic description of a collision between heavy ions is the time-dependent Hartree-Fock (TDHF) formalism or its extended version which includes the Boltzmann collision term.

The semiclassical microscopic approximations to these extended mean-field theories in a form of a Boltzmann-Uehling-Uhlenback (BUU), Vlasov-Uehling-Uhlenback (VUU), Boltzmann-Nordheim-Vlasov (BNV), or Landau-Vlasov equations are relatively easier to solve and have been extensively used to describe various properties of nucleus-nucleus collisions [1, 4].

Since the extended TDHF formalism and its semiclassical analogs are all based on a mean-field approach, they are unable to adequately reproduce the experimentally observed large widths of distributions of many physical quantities. Various methods have been developed to incorporate fluctuations and many-body correlations into mean-field theories, as, for example, the time-dependent generator-coordinate method [5], the variational approach with time-dependent observables [6], stochastic TDHF [7], etc. Relatively recently the Boltzmann-Langevin equation, which can be derived from the stochastic TDHF formalism [7], has been studied in the semiclassical formalism. In these calculations a fluctuating Langevin force is added to the Boltzmann collision term [8, 9]. This method is very promising but relatively complicated and computationally time consuming. A similar approach has been used by the authors of Ref. [10], and recently some numerical simulations have been performed [11]. Two different ways of calculating dispersions have been used in Ref. [2]: a semiclassical analog to the variational treatment of Balian and Veneroni [6] and a method of restoring classical many-body correlations in Vlasov and Landau-Vlasov dynamics. This last approach is used in the present paper to calculate second moments of various distributions.

The motivation for using a classical macroscopic trajectory calculation with one-body dissipation to describe the reaction ^{98}Mo + ^{98}Mo at the energy of 14.7 MeV/nucleon stems from the success of this model in predicting fusion and incomplete fusion cross sections

[12] and in analyzing many of the observed properties of strongly damped collisions in the low-energy regime (below 10 MeV/nucleon) [13,14]. Several methods have been developed to evaluate second moments for these kinds of calculations in the framework of collective transport models [9]. The most commonly used are based on the Fokker-Planck equation [9,15] or on Monte Carlo simulations. Because of the unsatisfactory agreement between the macroscopically calculated first moments and the experimantal data, we did not proceed with an evaluation of the second moments within this framework.

In Sec. II we describe the microscopic and macroscopic models used in our investigation. Next, in Sec. III, we discuss the first moments of various distributions and compare the predictions of the microscopic and macroscopic models. Section IV is devoted to an analysis of second moments obtained from the microscopic model. Finally, we summarize our results and present our conclusions in Sec. V.

II. THEORY

In this section we summarize the ingredients of the microscopic and macroscopic models which we use.

The microscopic approach has its origins in the Wigner transform of the TDHF equations of motion. Including only terms up to second order in $\hbar$ leads to the Vlasov equation for the one body distribution function $f(\mathbf{r},\mathbf{p},t)$:

$$\frac{\partial f}{\partial t}+\frac{\mathbf{p}}{m}\boldsymbol{\nabla}_{\mathbf{r}}f-\boldsymbol{\nabla}_{\mathbf{r}}U\boldsymbol{\nabla}_{\mathbf{p}}f=0. \tag{1}$$

Here $\mathbf{r}$ and $\mathbf{p}$ represent the space and momentum coordinates. The single-particle potential U is treated in a self-consistent manner. If, in addition to the one body potential U, one includes the residual two-body interaction by incorporating a collision term $I_{\rm coll}$, one may write the Landau-Vlasov equation in the form

$$\frac{\partial f}{\partial t}+\frac{\mathbf{p}}{m}\boldsymbol{\nabla}_{\mathbf{r}}f-\boldsymbol{\nabla}_{\mathbf{r}}U\boldsymbol{\nabla}_{\mathbf{p}}f=I_{\rm coll}. \tag{2}$$

The collision term is calculated using an effective nucleon-nucleon cross section which is consistent with the requirements of energy and momentum conservation and with Pauli blocking [1]. The effective nucleon-nucleon cross section is deduced from the free, energy-dependent, cross section according to

$$\left(\frac{d\sigma}{d\Omega}\right)^{\rm eff}_{NN}=\left(\frac{d\sigma}{d\Omega}\right)^{\rm free}_{NN}Y(\rho), \tag{3}$$

where $Y(\rho)$ is a density scaling factor suggested by Lejeune *et al.* [16]. The Landau-Vlasov equation is solved by expressing the distribution function $f(\mathbf{r},\mathbf{p},t)$ as a linear combination of the distribution functions for a large number N of pseudoparticles:

$$f(\mathbf{r},\mathbf{p},t)=\sum_{i=1}^{N}w_i(\mathbf{r},\mathbf{p})\,f_i(\mathbf{r},\mathbf{r}_i,\mathbf{p},\mathbf{p}_i,t). \tag{4}$$

The pseudoparticle distributions are expressed as uncorrelated isotropic Gaussian wave packets:

$$f_i(\mathbf{r},\mathbf{r}_i,\mathbf{p},\mathbf{p}_i,t)=\frac{1}{N}\left(\frac{1}{\sqrt{2\pi\sigma_r^2}\sqrt{2\pi\sigma_p^2}}\right)\times\exp\left\{-\frac{(\mathbf{r}-\mathbf{r}_i)^2}{2\sigma_r^2}-\frac{(\mathbf{p}-\mathbf{p}_i)^2}{2\sigma_p^2}\right\}. \tag{5}$$

The centroids of the Gaussian wave packets are given by $\mathbf{r}_i(t)$ and $\mathbf{p}_i(t)$. The widths of these Gaussian wave packets are kept constant in time and are determined by requiring that the binding energy and mean square radius of the ground-state nucleus are correctly described [1]. The decomposition of the distribution into Gaussians is useful for numerical calculations since it assures a smooth distribution of density within the nuclear system. It corresponds to an extension of the Thomas-Fermi approximation and therefore accounts for some of the quantum effects at the level of that approximation. The weight factors w_i in Eq. (4) are treated in the Thomas-Fermi approximation and are given by a step function

$$w_i=\Theta(\epsilon_f-\epsilon_i), \tag{6}$$

where ϵ_f denotes the Fermi energy and ϵ_i represents the mean single-particle energy for the pseudoparticle state. The positions and the momenta of the N pseudoparticles are chosen randomly at time $t=0$ within the available phase space determined by using Eq. (6). The dynamical evolution of the system is obtained by following the semiclassical trajectories of these pseudoparticles. For the self-consistent mean field we use a simplified Skyrme interaction consistent with the compressibility modulus $\kappa=200$ MeV [1,17].

It is important to note that in the microscopic Landau-Vlasov approach there are no more free parameters which could be adjusted for a given reaction and energy.

The Landau-Vlasov equation is an equation for the average one-body distribution function. The fluctuations and many-body correlations are washed out, and fragments mass or charge distributions cannot be directly obtained from the solution of Eq. (2). Zielińska-Pfabé and Grégoire [2] have suggested a random sampling of a one-body distribution to construct "events" which were analyzed from the point of view of mass and charge distributions. This procedure, which is described below, is a way to reconstruct many-body correlations from the knowledge of the dynamical evolution of the one-body distribution. A very similar approach has been used more recently by Bonasera *et al.* [18], who looked at fragment formation within the one-body Boltzmann-Nordheim-Vlasov model.

Thus, to determine the dispersions of various quantities, such as mass or charge, we employ a procedure which restores the classical many-body correlations which are missing from the Landau-Vlasov approach. This method of restoring many-body correlations (RMBC) [2] treats the transport equations for the dispersions in a statistical fashion. It has been successfully used to determine

the mass and charge distributions for $^{16}O+^{16}O$ reaction [2].

The main procedure is as follows: Let Z_p and N_p be the numbers of protons and neutrons in the projectile and Z_t and N_t the corresponding numbers in the target nucleus. Among all pseudoparticles we now randomly choose Z_p and Z_t Gaussians which at time $t = 0$ correspond to the proton distribution in the projectile and target, respectively. Similarly, we choose N_p and N_t Gaussians which belonged to the neutron distribution in the projectile and target, respectively, at $t = 0$. We then follow their trajectories as determined by the Landau-Vlasov equation and identify them as belonging to the projectilelike fragment or the targetlike fragment on the basis of their positions at a given time t. In this procedure we discretize the occupation probability of these Gaussian states to 1 or 0, which corresponds to selecting a single Slater determinant out of a mixture of very many Slater determinants. This procedure is repeated for a very large number of combinations of Gaussians. Thus we simulate, in a statistical ensemble, the classical many-body correlations which are missing from the Landau-Vlasov formalism.

In the macroscopic approach we have performed a trajectory calculation in which we described the nuclear shape by using the parameterization of Błocki and Świątecki [3]. In this model a realistic description of the nuclear shape during the collision process is accomplished by using six collective variables. Three of these degrees of freedom correspond to the relative motion (ρ), the neck degree of freedom (λ), and the mass asymmetry (Δ). The other three correspond to the rotational degrees of freedom: the orbital angle (Θ) and the intrinsic angles of rotation for the two participating ions (ϕ_1 and ϕ_2). To determine the time evolution of these variables we solve a system of coupled Euler-Lagrange equations of motion [12, 19]:

$$\frac{d}{dt}\left[\frac{\partial T}{\partial \dot{q}_i}\right] - \frac{\partial T}{\partial q_i} = F_i^{\rm cons} + F_i^{\rm diss}. \tag{7}$$

For the symmetrical system $^{98}Mo+^{98}Mo$ we choose $\Delta = 0$ and are left with five collective variables $(q_1, q_2, q_3, q_4, q_5) = (\rho, \lambda, \Theta, \phi_1, \phi_2)$. The kinetic energy T is written as

$$T = \frac{1}{2}\sum_{i,j=1}^{2} T_{ij}\,\dot{q}_i\dot{q}_j + \frac{1}{2}I\dot{\Theta}^2 + \frac{1}{2}I_1\dot{\phi_1}^2 + \frac{1}{2}I_2\dot{\phi_2}^2, \tag{8}$$

where T_{ij} are the components of the inertia tensor for the collective motion and are determined using the Werner-Wheeler approximation to irrotational flow [20, 14]. The parameter-free Werner-Wheeler inertia tensor which is close to the one given by hydrodynamical model has been very successfully used in the past [14]. For I, I_1, and I_2 we use shape-dependent rigid-body moments of inertia. In Eq. (7), $F^{\rm cons}$ represents the components of the conservative forces and $F^{\rm diss}$ those of the dissipative forces. The conservative forces consist of the nuclear proximity and surface interactions [21] and of the Coulomb interaction. The Coulomb interaction has been calculated using the method of Beringer [22]. The one-body dissipative force consists of two parts, both linear in the collective velocities: the wall friction [23] and the window friction [24]. The forms and details of nuclear proximity and surface interactions, and the wall and window dissipation tensors are all standard and have been also used by many authors [12–15] before. Similarly to Landau-Vlasov model, the macroscopic method uses no free parameters.

III. RESULTS FOR THE FIRST MOMENTS

Using both models described in the previous section we studied the collision of $^{98}Mo + ^{98}Mo$ at an incident center-of-mass energy of 14.7 MeV per nucleon. Both of these parameter-free models allow us to follow, in detail, the time evolution of the colliding system and determine scattering angle and energy loss. When the Landau-Vlasov equation is solved one obtains the positions and momenta, at any time t, of all of the pseudoparticles which in turn determine the neutron and proton distributions of the entire interacting system. One may therefore calculate the position, momentum, kinetic energy, and potential energy of the system at any time. Similarly, using the macroscopic model, it is also possible, at any time, to determine these quantities. Thus, both models give us full information about the average values of various measurable quantities. However, since both of these models are based on mean-field approaches, they only contain information about the mean values (i.e., first moments) of the observables.

It has been suggested [25, 26] that the one-body dissipation rate as determined by the wall formula is too large by a factor of about 3. This is attributed to the neglect of quantum effects in this approach. Therefore, in this paper we also included some results from the macroscopic model where the one-body wall dissipation rate has been reduced by a factor of 3 as described in [19].

In Fig. 1 we show the calculated reaction times for the

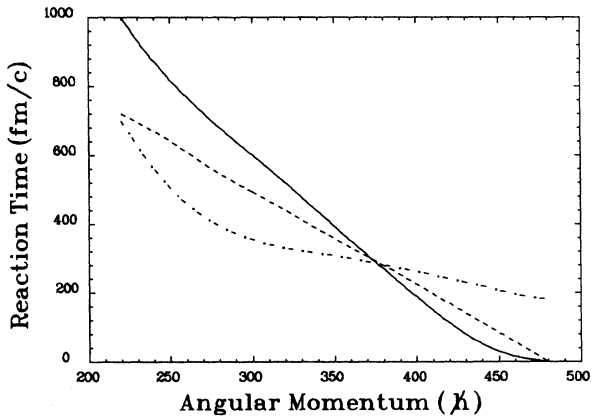

FIG. 1. Reaction time as a function of the relative angular momentum (in units of $\hbar$) for the reaction $^{98}Mo + ^{98}Mo$ at $E_{\rm c.m.} = 14.7$ MeV per nucleon. The solid line represents the results obtained with the macroscopic model. The dashed line was also obtained with the macroscopic model but with the strength of the one-body wall friction reduced as described in the text. Finally, the dot-dashed line shows the results obtained with the microscopic Landau-Vlasov model.

^{98}Mo + ^{98}Mo reaction as a function of incident angular momentum. The reaction time is determined here as the time from the moment when the ions touch in the entrance channel to the moment when their density distributions separate again in the exit channel. The solid line represents the results from the macroscopic model with full wall dissipation; the dashed line represents the results of the macroscopic model calculation with the one-body wall dissipation rate decreased as described above. Finally, the dot-dashed line represents the reaction times determined using the microscopic Landau-Vlasov model. Note that for peripheral collisions the microscopic calculations give longer reaction times than the macroscopic calculations. This occurs in part because the macroscopic calculations allow for dissipation due to the exchange of particles before the nuclei touch (the window friction). This friction damps out some of the relative motion and has the effect of reducing the reaction time because the nuclei are stopped before much overlap has occurred. Furthermore, in the macroscopic calculations there is a problem in getting a smooth transition of the inertias as the system changes from two separate nuclei to a single body. This difficulty leads to an overestimation of the dissipated energy for grazing collisions. Also, we see that for highly dissipative central collisions the reaction times obtained from the microscopic calculations are shorter than those obtained from the macroscopic calculations. This is again caused by the stronger friction used in the macroscopic model. The effect of friction on the reaction time is clearly demonstrated by the shortening of this time that is obtained by reducing the strength of the wall dissipation in the macroscopic calculation (dashed line).

The total kinetic energy (TKE) of the outgoing fragments is shown in Fig. 2 where the results of the macroscopic calculations and the microscopic calculations are compared with the experimental data of [27] (the dotted line). Again, the solid line represents the results of the macroscopic model; the dot-dashed line represents the TKE determined with the microscopic model. Both calculations indicate that the reaction is overdamped for small impact parameters. It is interesting to note that the experimentally determined TKE indicates that these reactions may not be overdamped. For more peripheral reactions the macroscopic calculations yield a much larger energy dissipation than the microscopic model. For this range of large impact parameters the microscopic calculations agree very well with the experimental data.

The deflection function for the above reaction was studied and the results are presented in Fig. 3. Here, the solid line represents the results of the macroscopic model, the dashed line represents the results of the macroscopic model with reduced one-body wall friction, and the dot-dashed line represents the scattering angle determined using the microscopic model. The microscopic calculation was performed only for angular momentum l larger than 200. Below this value the reaction time increases very rapidly (see Fig. 1), which makes the computing time inhibitly long. We observe that for central collissions the model predicts too much energy dissipation and the interacting ions get to a state of "quasifusion." We believe that the reduction of the free nucleon-nucleon cross section [16] which determines the Boltzmann collision term [1] might not be sufficient for the high density overlap which occurs for low impact parameters. Experimental results from [27] are also shown in Fig. 3 as a dotted line. The authors of this reference used a parametrization of the deflection function suggested by Wolschin and Nörenberg [28] to calculate the deflection angle as a function of angular momentum or energy loss. The Landau-Vlasov results agree better with the experimental results than do the macroscopic results. The de-

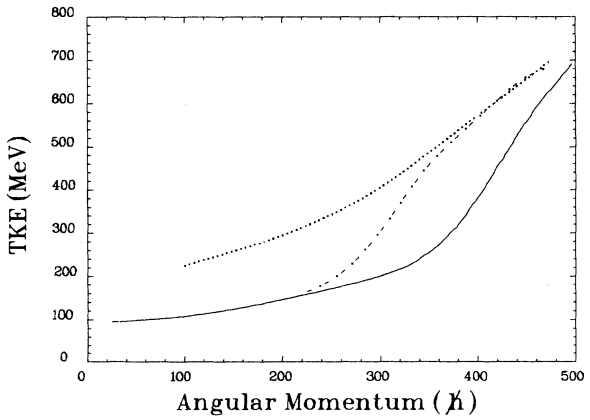

FIG. 2. Total kinetic energy of the outgoing fragments as a function of their relative angular momentum (in units of $\hbar$) for the reaction ^{98}Mo + ^{98}Mo at $E_{\text{c.m.}}$ = 14.7 MeV per nucleon. The solid line represents the results obtained with the macroscopic model. The dot-dashed line shows the results obtained with the microscopic Landau-Vlasov model. The dotted line represents the experimental results discussed in the text.

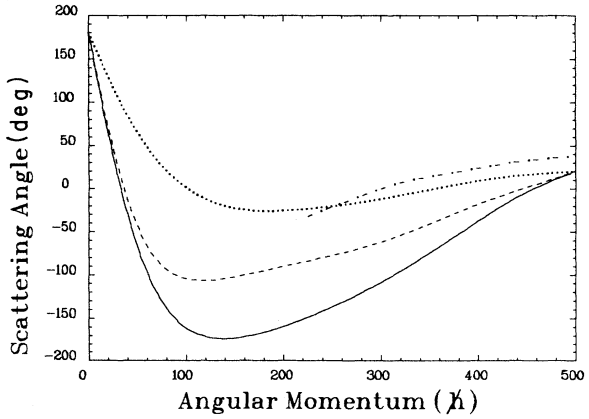

FIG. 3. Deflection function for the reaction ^{98}Mo+^{98}Mo at $E_{\text{c.m.}}$ = 14.7 MeV per nucleon. The solid line represents the results obtained with the macroscopic model. The dashed line was also obtained with the macroscopic model but with the strength of the one-body wall friction reduced as described in the text. The dot-dashed line shows the results obtained with the microscopic Landau-Vlasov model. The dotted line represents the experimental results discussed in the text.

flections predicted by the macroscopic model correspond to too negative scattering angles. The large deflections observed in the macroscopic calculations are caused by longer reaction times and are consistent with the results presented in Fig. 1.

IV. SECOND MOMENTS

One of the most interesting features observed in heavy ion reactions is the existence of large dispersions in observables such as mass, charge, or scattering angle. Hence, we study the second moments of these observables using the microscopic RMBC model discussed in Sec. II. We use this procedure to determine the mass dispersion, the charge dispersion, and the dispersion in the scattering angle for the ^{98}Mo+^{98}Mo reaction studied in Sec. III.

To study the dispersions we first calculate the variances in mass, charge, and scattering angle for various impact parameters. We then construct dispersion plots (contour plots of double differential cross sections) for the charge dispersion, the mass dispersion, and the dispersion in the scattering angle (Wilczyński plot). For example, for the mass distribution we have

$$\frac{d^2\sigma}{dE\,dA} = C\int_{b_{\min}}^{b_{\max}} \exp\left\{-\frac{(E-E_b)^2}{2\sigma_{E,b}^2} - \frac{(A-A_b)^2}{2\sigma_{A,b}^2}\right\} b\,db, \qquad (9)$$

where the integration is over the impact parameter, E is the TKE, A is the mass number of a projectilelike fragment, and E_b is the mean value of the TKE for a given impact parameter b. A_b is the mean value of the mass for a given impact parameter b, and $\sigma_{E,b}$ and $\sigma_{A,b}$ are the variances in the TKE and the mass of the projectile for a given b. The normalization constant C is chosen so that the total deep inelastic cross section is given by $\sigma = \int_{b_{\min}}^{b_{\max}} b\,db$, with $b_{\min} = 5.5$ fm and $b_{\max} = 11.5$ fm. The double differential cross sections $\frac{d^2\sigma}{dE\,dZ}$ and $\frac{d^2\sigma}{dE\,d\Theta}$ are determined in a similar fashion.

The Wilczyński plot ($\frac{d^2\sigma}{dE\,d\Theta}$) for the reaction ^{98}Mo+^{98}Mo at $E_{\rm c.m.} = 14.7$ MeV per nucleon is shown in Fig. 4. We use ten contours for the range of cross sections from 0 to 230 mb/(MeV deg). The most important feature of this plot is the shape of the ridge as it bends to negative angles for large energy losses. The double differential cross section $\frac{d^2\sigma}{dE\,dA}$ is shown in Fig. 5 where we have again used ten contours to display the range 0–66 mb/(MeV A). The shift of the mean of the distribution from the expected value of 98 results from a mass loss caused by the evaporation of pseudoparticles from the hot nuclei. It is clear from this figure that for highly dissipative reactions the dispersion is enhanced. This is also evident in Fig. 6, which shows the double differential cross section $\frac{d^2\sigma}{dE\,dZ}$ in the range 0–70 mb/(MeV Z). This graph also shows a shift in the mean due to evaporation.

To compare our calculated dispersions with the experimental results of Ref. [27], we need to determine the variances $\sigma_{E,b}$ and $\sigma_{A,b}$ as functions of the TKE loss (TKEL). The procedure used here is equivalent to making cuts in the plots for $\frac{d^2\sigma}{dE\,dZ}$ or $\frac{d^2\sigma}{dE\,dA}$ at a given value of TKEL and finding the first and second moments of these distributions. For example, the average value of the mass number and its variance for a given value of TKEL are

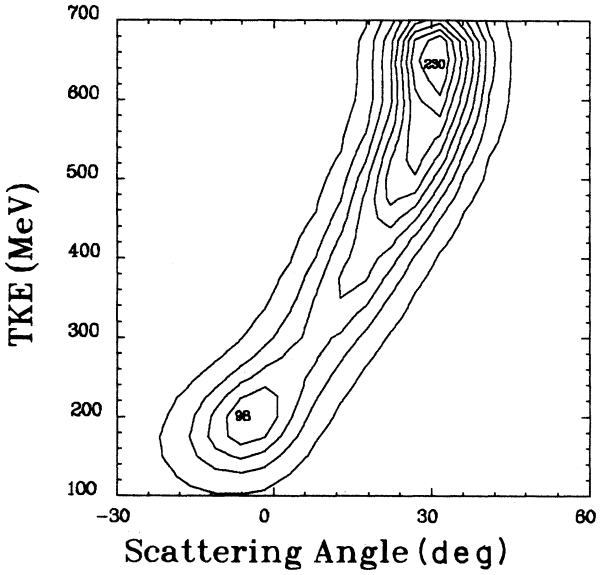

FIG. 4. Wilczyński plot ($\frac{d^2\sigma}{dE\,d\Theta}$) for the reaction ^{98}Mo+^{98}Mo at $E_{\rm c.m.} = 14.7$ MeV per nucleon obtained by Landau-Vlasov and RMBC methods. The maximum value at the peak was 230 mb/(MeV deg).

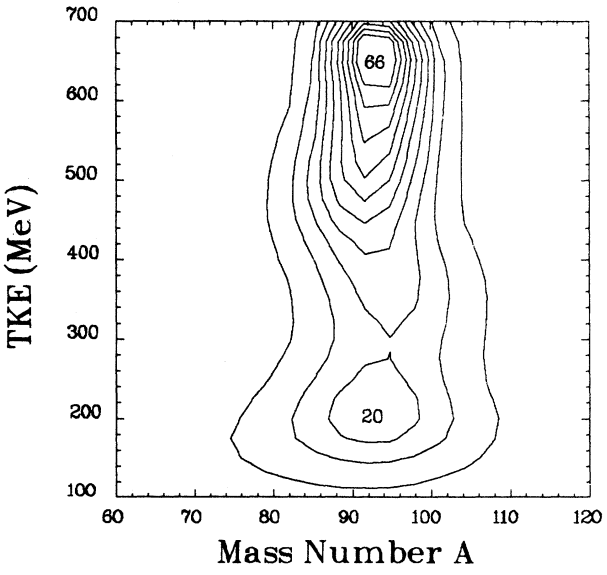

FIG. 5. Double differential cross section ($\frac{d^2\sigma}{dE\,dA}$) for the reaction ^{98}Mo+^{98}Mo at $E_{\rm c.m.} = 14.7$ MeV per nucleon obtained by using Landau-Vlasov and RMBC methods. The maximum value at the peak was 66 mb/(MeV A).

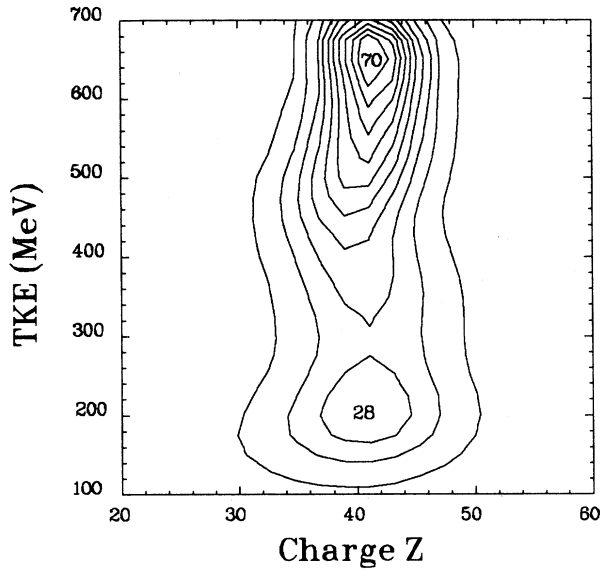

FIG. 6. Double differential cross section ($\frac{d^2\sigma}{dE\,dZ}$) for the reaction ^{98}Mo+^{98}Mo at $E_{\rm c.m.}$ = 14.7 MeV per nucleon obtained by using Landau-Vlasov and RMBC methods. The maximum value at the peak was 70 mb/(MeV Z).

$$\bar{A} = \left(\frac{\sum_A A \left(\frac{d^2\sigma}{dE\,dA} \right)}{\sum_A \left(\frac{d^2\sigma}{dE\,dA} \right)} \right)_{E=\text{TKEL}} \tag{10}$$

and

$$\sigma_A^2 = \left(\frac{\sum_A (\bar{A} - A)^2 \left(\frac{d^2\sigma}{dE\,dA} \right)}{\sum_A \left(\frac{d^2\sigma}{dE\,dA} \right)} \right)_{E=\text{TKEL}} \tag{11}$$

Here the summations are performed over the cuts E=TKEL. A similar procedure is employed to determine the first and second moments of the charge distribution. Since we were not able to perform microscopic calculations for very central collisions where one could expect an enhancement of dispersions, the method of finding the dispersions for a given TKEL described above could lead to some underestimations for large values of TKEL. We have also found that since the values of the widths of TKE are large, the dispersions in mass and charge for TKEL which are comparable with these widths are spuriously enhanced by the results obtained for larger TKEL. For this reason we did not calculate mass and charge dispersions for TKEL below 75 MeV.

Since in the Landau-Vlasov formalism the positions of all pseudoparticles are known at any time, we also determine for each collision the number of neutrons or protons which are exchanged during the reaction and compare this quantity to the variances determined by the RMBC method.

Figure 7 shows σ_A^2 as a function of TKEL for the ^{98}Mo + ^{98}Mo reaction which we studied. The dots with error bars show the experimental data from Ref. [27], the solid line is the RMBC prediction, and the dashed line is the number of exchanged nucleons. Our results do not agree with the experimental analysis especially for large

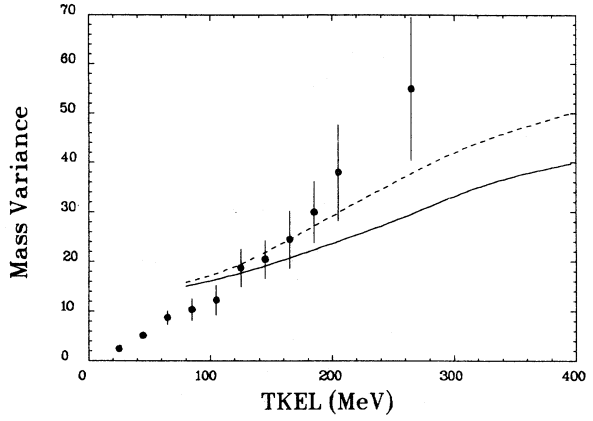

FIG. 7. Mass variance as a function of total kinetic energy loss for the reaction ^{98}Mo+^{98}Mo at $E_{\rm c.m.}$ = 14.7 MeV per nucleon. The data points represent experimental results from Ref. [27]. The solid line is the RMBC prediction, and the dashed line is determined from the number of exchanged nucleons as discussed in the text.

TKEL where the experimental mass variances are very large. It is also clear from this figure that the number of nucleons exchanged during the reaction (dashed line) exhibits the properties of collective transport theories, in other words, a proportionality to the mass variances. This relationship is expected as long as the drift is small.

The charge variance is shown in Fig. 8 along with the number of exchanged protons. Once again the solid line is the RMBC result, the dashed line is the number of exchanged protons, and the dots with error bars are the data from Ref. [27]. Here the variances predicted by the RMBC method are closer to the experimental results, but there is still a systematic discrepancy for small TKEL.

Finally, in Fig. 9 we show the mass variance, as deter-

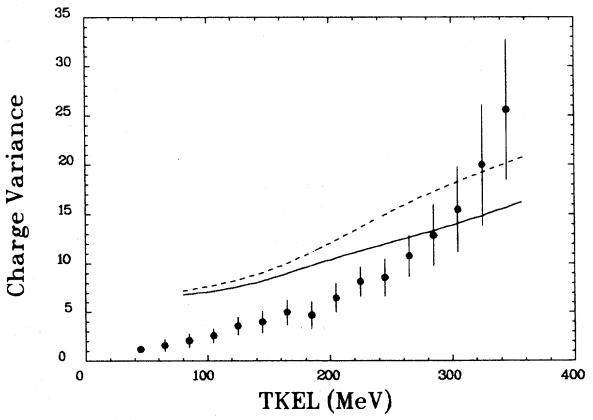

FIG. 8. Charge variance as a function of total kinetic energy loss for the reaction ^{98}Mo+^{98}Mo at $E_{\rm c.m.}$ = 14.7 MeV per nucleon. The data points represent experimental results from Ref. [27]. The solid line is the RMBC prediction, and the dashed line is determined from the number of exchanged nucleons as discussed in the text.

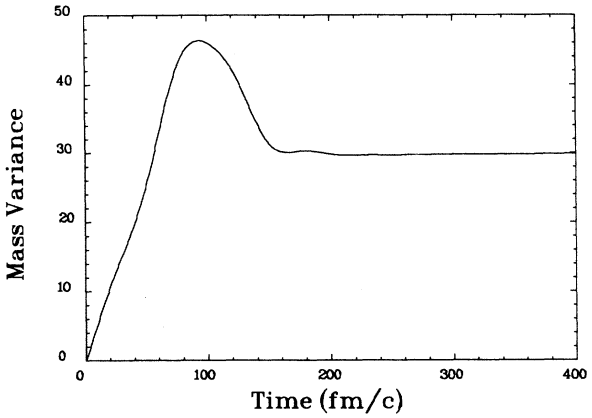

FIG. 9. Mass variance plotted as a function of time. The reaction is ^{98}Mo + ^{98}Mo at $E_{\text{c.m.}}$ = 14.7 MeV per nucleon with an impact parameter of 8.5 fm obtained by using Landau-Vlasov and RMBC methods.

mined by the RMBC method, plotted as a function of time for the reaction ^{98}Mo+^{98}Mo at $E_{\text{c.m.}}$ = 14.7 MeV per nucleon and impact parameter of 8.5 fm. The large peak at around 100 fm/c for the RMBC result is a sign of dynamical correlations which occur during the collision and which die out with time.

V. SUMMARY AND CONCLUDING REMARKS

We have studied the reaction ^{98}Mo + ^{98}Mo at $E_{\text{c.m.}}$ = 14.7 MeV per nucleon with both microscopic and macroscopic mean-field theories. For the microscopic model we used a Landau-Vlasov semiclassical approach which includes a residual interaction in the form of a two-body collision term. For the macroscopic model we used a collective model approach which included one-body wall and window dissipation. Both of these models were used to study the reaction time, TKE, and scattering angle as functions of the incident angular momentum. Additionally, within the framework of the microscopic Landau-Vlasov model we have calculated the dispersions in charge, mass, and scattering angle, using the method described in Ref. [2].

We have demonstrated that the reaction times obtained with the macroscopic model for more central collisions are much longer than predicted by Landau-Vlasov calculations. This is because the wall friction was too strong, mainly during the initial stages of the reaction. This made the deflection angle too negative as compared to the experimentally observed values. The scattering angles obtained with the Landau-Vlasov model which contains a residual-interaction collision term agree much better with the experimental results.

We would like to stress here that for central collisions the experimentally determined TKEL of the outgoing fragments was systematically smaller than that predicted by both the microscopic and collective models. In other words, both theoretical models predict considerably more dissipation for central collisions than is experimentally observed. Therefore, in the case of the macroscopic approach some reduction of the one-body wall friction is necessary. In the case of the microscopic model we believe that a further reduction of the free nucleon-nucleon cross section is important, especially for the high density overlap.

We found that for large TKEL the Landau-Vlasov dynamics with a two-body collision term and with the RMBC method underestimates the large and exponentially increasing mass variances deduced from experiments presented in [27]. The inclusion of quantum mechanical fluctuations might be quite important, especially for central collisions.

The calculated charge variances are larger than the observed ones (except above a TKEL of 300 MeV). The agreement with the experimental charge variances might be improved by including a further refinement of the isospin interaction term [29] in the Landau-Vlasov formalism.

ACKNOWLEDGMENTS

One of us (M.Z.-P.) would like to acknowlege the warm hospitality of GANIL Laboratory where the microscopic calculations were started.

[1] Ch. Grégoire, B. Rémaud, F. Sébille, L. Vinet, and Y. Raffray, Nucl. Phys. **A465**, 317 (1987).
[2] M. Zielińska-Pfabé and Ch. Grégoire, Phys. Rev. C **37**, 2594 (1988).
[3] J. Błocki and W.J. Świątecki (unpublished).
[4] G.F. Bertsch and S. Das Gupta, Phys. Rep. **160**, 189 (1988), and references therein; J. Aichelin and G.F. Bertsch, Phys. Rev. C **31**, 1730 (1985).
[5] P.G. Reinhard, R.Y. Cusson, and K. Goeke, Nucl. Phys. **A398**, 141 (1983).
[6] R. Balian and M. Veneroni, Ann. Phys. (N.Y.) **135**, 270 (1981); J.M. Marston and S. Koonin, Phys. Rev. Lett. **54**, 1139 (1985).
[7] P.G. Reihard and E. Suraud, Ann. Phys. (N.Y.) **215**, 98 (1992).
[8] S. Ayik and Ch. Grégoire, Phys. Lett. B **212**, 269 (1988); Nucl. Phys. **A513**, 187 (1990); E. Suraud, S. Ayik, M. Belkacem, and J. Stryjewski. *ibid.* **A542**, 141 (1992).
[9] S. Ayik, E. Suraud, J. Stryjewski, and M. Belkacem, Z. Phys. A **337**, 413 (1990), and references therein.
[10] J. Randrup and B. Rémaud, Nucl. Phys. **A514**, 339 (1990).
[11] Ph. Chomaz, G.F. Burgio, and J. Randrup, Phys. Lett. B **254**, 340 (1991).
[12] D. Sperber, J. Stryjewski, and M. Zielińska-Pfabé, Phys. Scri. **36**, 880 (1987), and references therein.
[13] J.N. De, D.H.E. Gross, and H. Kalinowski, Z. Phys. A **277**, 385 (1976); H.H. Deubler and K. Dietrich, Nucl.

Phys. **A277**, 493 (1977); F. Beck, J. Błocki, and M. Dworzecka, Phys. Lett. B **76**, 35 (1978).
[14] S.K. Samaddar, M.I. Sobel, J.N. De, S.I.A. Garpman, D. Sperber, and M. Zielińska-Pfabé, Nucl. Phys. **A332**, 210 (1979); D. Sperber and J. Stryjewski, Nucl. Phys. **A505**, 471 (1989).
[15] S.K. Samaddar, D. Sperber, M. Zielińska-Pfabé, M.I. Sobel, and S.I.A. Garpman, Phys. Rev. C **23**, 760 (1981).
[16] A. Lejeune, P. Grangé, M. Martzolff, and J. Cugnon, Nucl. Phys. **A453**, 189 (1986).
[17] J.N. Negele, Rev. Mod. Phys. **54**, 913 (1982); S. Levit and P. Bonche, Nucl. Phys. **A437**, 426 (1985).
[18] A. Bonasera, M. Colonna, M. Di Toro, F.Gulminelli, and H.H. Wolter, Phys. Lett. B **244**, 169 (1990).
[19] D. Sperber, J. Stryjewski, and M. Zielińska-Pfabé, Phys. Lett. B **197**, 507 (1987).
[20] J.A. Wheeler (private communication).
[21] J. Błocki, J. Randrup, and W.J. Świątecki, Ann. Phys. (N.Y.) **105**, 427 (1977).
[22] R. Beringer, Phys. Rev. **131**, 1402 (1963).
[23] J. Błocki, Y. Boneh, J.R. Nix, J. Randrup, A.J. Sierk, and W.J. Świątecki, Ann. Phys. (N.Y.) **113**, 330 (1978).
[24] J. Randrup, Ann. Phys. (N.Y.) **112**, 356 (1978).
[25] J.R. Nix, in Proceedings of the IV Workshop on Nuclear Dynamics, Copper Mountain, Colorado, 1986 [University of Indiana Report Nos. CONF-860270, UC-34C, and INC-40007-37 (National Technical Information Service, U.S. Department of Commerce)], p. 1.
[26] J.J. Griffin, in [25], p. 5.
[27] M. Petrovici, J. Albiński, R. Bock, R. Cusson, A. Gobbi, G. Guarino, S. Gralla, K.D. Hildenbrand, W.F.J. Müller, A. Olmi, H. Stelzer, and J. Töke, Nucl. Phys. **A477**, 277 (1988).
[28] G. Wolschin and W. Nörenberg, Z. Phys. A **284**, 209 (1978).
[29] M. Farine, T. Sami, B. Rémaud, and F. Sébille, Z. Phys. A **339**, 363 (1991).